Unintentional conductivity of indium nitride: transport modelling and microscopic origins

Unintentional conductivity of indium nitride: transport modelling and microscopic origins

P D C King, T D Veal and C F McConville

Department of Physics, University of Warwick, Coventry CV4 7AL, UK

E-mail: C.F.McConville@warwick.ac.uk

Abstract
A three-region model for the high n-type conductivity in InN, including contributions from the bulk, surface and buffer layer interface of the sample, is considered. In particular, a parallel conduction analysis is used to show that this model can account for the carrier concentration and mobility variation with film thickness that has previously been determined from single-field Hall effect measurements. Microscopic origins for the donors in each region are considered, and the overriding tendency towards n-type conductivity is discussed in terms of the bulk band structure of InN.

1. Introduction

Indium nitride (InN) has been the subject of intense research in recent years. Some of its most attractive features are its excellent predicted transport properties such as high electron mobilities [1], a small band edge electron effective mass, high peak drift velocities [2], and high frequency transient drift velocity oscillations [3]. These suggest enormous potential application for InN in high frequency electronic devices, such as field-effect transistors operating up to the terahertz range. In order to achieve optimal transport characteristics, low carrier densities are required. However, every undoped InN sample grown to date exhibits a high unintentional n-type conductivity, which it is important to understand and control if InN's potential for use in device applications is to be realized. In this article, general features of conductivity in InN are reviewed, and new modelling is introduced. In particular, a parallel conduction treatment of single-field Hall effect results in InN is presented, including contributions from the bulk, surface and interface regions of InN samples.

Early work on InN was largely performed on samples grown by sputter deposition. The resulting films were generally polycrystalline with extremely high electron densities ($n \sim 10^{20}$ cm^{-3}) and low Hall mobilities ($\mu \lesssim 100$ cm^2 V^{-1} s^{-1}) [4]. Such high carrier concentrations result in the Fermi level lying well above the conduction band minimum (CBM) in InN. Consequently, a large Moss–Burstein [5, 6] shift was present in optical absorption

measurements performed on such samples, causing the fundamental band gap of InN to be wrongly assigned at almost 2 eV [7]. However, a notable reduction in carrier density and increase in mobility were obtained when high quality single-crystalline films of InN were grown by alternative methods such as plasma-assisted molecular beam epitaxy (PAMBE) [8, 9] and metal-organic vapour-phase epitaxy (MOVPE) [9, 10], revealing potential in the transport properties of this material. This improvement in growth also allowed a revision of the fundamental band gap of InN to $\sim$0.7 eV [9, 11–14], extending the spectral range spanned by the III–N semiconductors from the ultraviolet and visible into the infrared, suggesting application of In-containing III–N compounds in a wide range of optoelectronic devices such as full solar spectrum photovoltaics [15], high-performance light-emitting and laser diodes [16–18] and solid-state lighting [19].

InN has also been suggested as a suitable material for light emission in the terahertz frequency range [20], with emission intensities already reported that exceed those from p-type InAs [21], which was previously thought to be the most efficient terahertz emitter. Further increases in emission intensity have recently been reported for a-plane InN [22] and from InN nanorod arrays [23]. InN has also shown potential for use as a chemical sensing device, with a chemically selective 'fast capture, slow response' modification of its electrical properties observed upon exposure to a number of solvents [24], and it has been proposed as a suitable material for biological sensing applications [25] and for

anion concentration measurements [26, 27]. This wide range of potential device applications has stimulated a large and sustained research effort, not least in materials synthesis, with optimization of growth conditions, substrate choices and buffer layer structures all being performed [28–34], with the best samples currently exhibiting free-electron densities of $\sim 3 \times 10^{17}$ cm^{-3} and mobilities over 2000 cm^2 V^{-1} s^{-1}, from single-field Hall effect measurements. However, non-parabolic carrier statistics calculations give the Mott density as $n_{\mathrm{m}} \approx 2 \times 10^{17}$ cm^{-3}, and so unintentionally doped InN samples still exhibit degenerate n-type conductivity, which requires further investigation.

Additionally, these superior electrical properties have only been achieved in thick InN films, with a marked increase (decrease) observed in volume electron concentration (mobility), determined from single-field Hall effect measurements, with decreasing film thickness [28, 29, 35, 36], shown for samples grown by PAMBE on GaN buffer layers in figure 1. The sheet density determined from single-field Hall effect measurements of a number of samples grown by PAMBE on both GaN and AlN buffer layers [37, 38] and of both In-and N-polarity [30, 31] showed a linear dependence on film thickness, suggesting that the true 'bulk' carrier density does not vary with thickness of the film. However, the linear relation does not extrapolate to zero density at zero thickness, indicating that there is some 'excess' conduction mechanism that must also be considered in InN, attributed to electron accumulation at the surface and/or interface [38]. This is consistent with multiple-field Hall effect measurements, which indicate at least two types of carriers of differing mobility in InN samples [39–41], consistent with 'bulk' electrons, and electrons in a surface and/or interface electron accumulation region.

The constant 'bulk' density has been estimated from the slope of the sheet density as a function of film thickness to be $\sim 4 \times 10^{17}$ cm^{-3} for In-polar InN grown under In-rich conditions on a GaN template [30]. For a sufficiently thick sample, any contribution from a surface or interface electron accumulation region would be expected to be negligible when averaged over the (large) film thickness, and so the volume electron concentration determined from a single-field Hall effect measurement should also approach the true bulk density as the film thickness becomes large. Using this method, a bulk density of $n \sim 3 \times 10^{17}$ cm^{-3} can be estimated from figure 1(a), in good agreement with that determined from the gradient of the sheet density versus film thickness. This is also in agreement with the bulk electron density determined from multiple-field Hall effect measurements on a 7.5 μm thick InN sample [39]. However, it is clear from figure 1 that this represents just one contribution to the total conductivity: it is also necessary to include other mechanisms when considering conductivity in InN.

2. Surface electron accumulation

To investigate whether a surface electron accumulation could be the cause of the 'excess' sheet density determined from single-field Hall effect measurements, Lu *et al* [38] performed electrochemical capacitance–voltage measurements, revealing
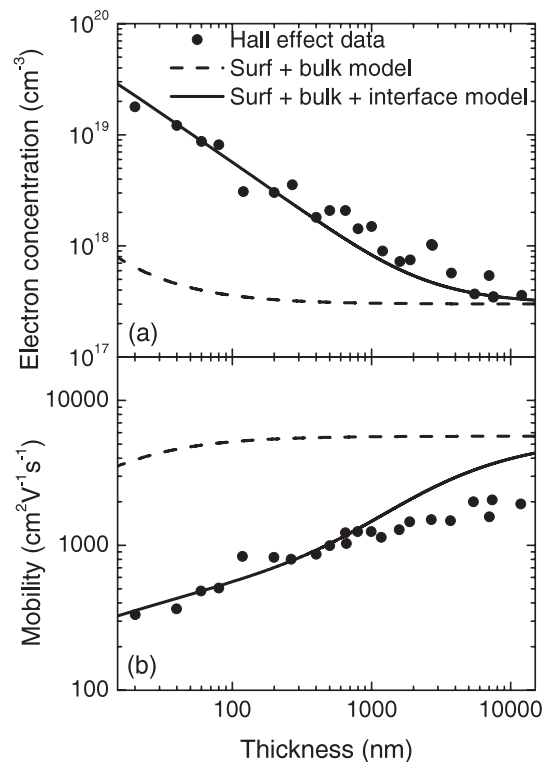

Figure 1. (a) Volume electron concentration and (b) mobility determined by single-field Hall effect measurements of a number of InN samples of varying thickness grown by PAMBE on GaN buffer layers on sapphire substrates [28, 29]. A parallel conduction model, described in the text, considering bulk and surface (dashed line) and additionally interface (solid line) contributions is also shown.

that a pronounced increase in electron density occurs close to the surface, in contrast to all other III–V semiconductors except for InAs [42], which exhibit a depletion of electrons at the surface. Mahboob *et al* [43] performed high-resolution electron energy loss spectroscopy measurements on clean surfaces, directly probing the conduction band plasma in the near surface region and confirming such an electron accumulation as an intrinsic property of InN. The electron accumulation is accompanied by a large downward bending of the conduction and valence bands relative to the Fermi level, with the Fermi level at the surface being pinned well above the CBM, as shown in figure 2.

Subsequent investigations have confirmed that this electron accumulation is present at the surface of both clean [44, 45] and oxidized [46–49] InN. In addition to the In-polar *c*-plane surface, on which most previous investigations have focused, a pronounced universality of the degree of electron accumulation has been observed for both In- and N-polar *c*-plane and non-polar *a*-plane InN [44], with the Fermi level being pinned 1.53 eV above the valence band maximum (VBM) in each case, and a surface state density of $N_{\mathrm{s}} \approx 1.65 \times 10^{13}$ cm^{-2}. In addition, electron accumulation has also been observed at the non-polar *m*-plane surface of InN nanocolumns [50, 51] and the zinc-blende InN(001) surface [44]. In fact, the only InN surface on which an absence of electron accumulation has been observed is the non-polar
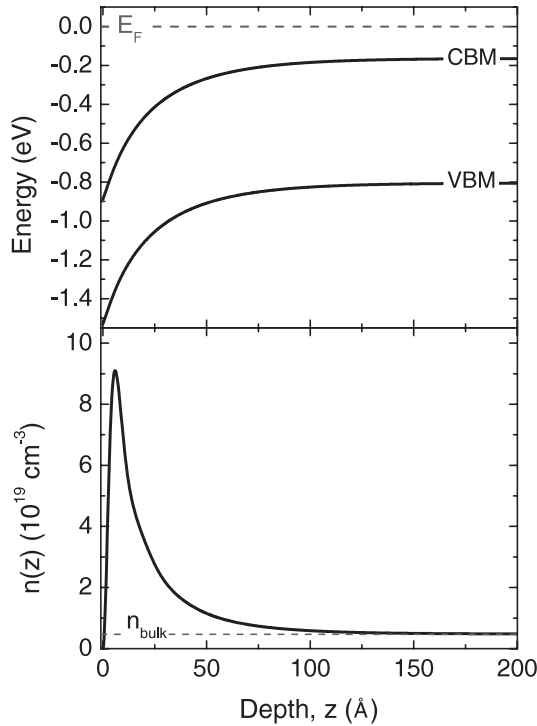
Figure 2. (a) Band bending and (b) variation of electron concentration in the accumulation layer at an InN surface, for an effective bulk concentration of $n \approx 5 \times 10^{18}$ cm^{-3} and surface Fermi level pinning position 1.53 eV above the VBM [44].

a-plane surface prepared by a perfect cleave in ultra-high vacuum [52]. Indeed, this is the same situation as for all III–V semiconductors [53, 54], including InAs, which exhibit flat-bands (no surface space–charge) following a perfect *in vacuo* cleave resulting in no step edges or contamination. It does not, however, represent a practical way to provide an InN surface without electron accumulation for use in device applications.

An accumulation of electrons at the as-grown, *ex situ* prepared or oxidized surface explains why metal contacts to InN have been found to exhibit almost exclusively Ohmic behaviour [38, 55]. However, this also provides a mechanism for a variation in average electron concentration with film thickness as the surface electron accumulation contributes a constant sheet density, independent of the film thickness. To investigate the effect of this on the single-field Hall results, a parallel conduction analysis [56, 57] has been performed, where the Hall sheet density, N_{H}, and mobility, μ_{H}, satisfy

$$N_{\mathrm{H}}\mu_{\mathrm{H}} = N_{\mathrm{s}}\mu_{\mathrm{s}} + N_{\mathrm{b}}\mu_{\mathrm{b}} \qquad (1)$$

$$N_{\mathrm{H}}\mu_{\mathrm{H}}^{2} = N_{\mathrm{s}}\mu_{\mathrm{s}}^{2} + N_{\mathrm{b}}\mu_{\mathrm{b}}^{2} \qquad (2)$$

where N_{s} (N_{b}) and μ_{s} (μ_{b}) are the surface (bulk) sheet density and mobility, respectively. The surface sheet density is taken as the universal value of $N_{\mathrm{s}} = 1.65 \times 10^{13}$ cm^{-2} [44], and the mobility of these surface electrons is estimated as $\mu_{\mathrm{s}} \approx 100$ cm^{2} V^{-1} s^{-1} from previous multiple-field Hall effect measurements [39]. The bulk volume density is taken as $n_{\mathrm{b}} = 3 \times 10^{17}$ cm^{-3} from the above discussions, and this is converted into a sheet density $N_{\mathrm{b}} = n_{\mathrm{b}}d$, where d is

the film thickness. The bulk carrier mobility was calculated from the ionized impurity scattering time calculated using the non-parabolic formalism of Zawadzki and Szymanska [58], as described elsewhere [59].

The results of this parallel conduction model are shown in figure 1 (dashed line). The electron concentration is clearly underestimated, and the mobility overestimated, for all thicknesses of sample. Even though very high carrier densities are present in the peak of the accumulation layer ($\sim 10^{20}$ cm^{-3}, figure 2), the band bending occurs over a distance approximately equal to the Thomas–Fermi screening length, with the bands returning to their bulk values within a distance typically of the order of 10 nm in InN. Consequently, the high carrier densities are very localized at the surface, and so do not contribute significantly to the measured electron density, except for very thin films. Additionally, as the carriers associated with the surface electron accumulation have a lower mobility than those in the bulk, their effect on the Hall effect measurements is reduced further. It should be noted, however, that even if the mobilities of the surface electrons are assumed to be as high as that of the bulk electrons, this model is still insufficient to reproduce the variation in measured electron density with film thickness [35]. Another explanation is therefore required to explain the single-field Hall effect results. The exception to the above discussions is for p-type InN, where the electron accumulation creates an inversion layer at the surface [57, 60, 61], and the p-type bulk is separated from an n-type surface region by a depletion layer. In this case, the n-type surface region dominates the single-field Hall effect measurements, which consequently indicate n-type conductivity even if the bulk of the sample is p-type [57].

3. Interface-related electron density

InN has a large lattice mismatch with typical substrate and buffer layer materials, for example 11% and 14% with GaN and AlN, respectively. Consequently, the InN/buffer layer interface is characterized by a large number of strain-relieving threading dislocations (TDs), whose density falls off exponentially with distance from the interface [62–65]. By analogy with GaN [66], charged dislocation scattering was suggested as a mechanism to explain the reduction in mobility with decreasing film thickness [28]. However, dislocations in GaN are known to act as acceptors, and this was originally assumed to be the case for InN also [62], and so this mechanism was not thought to explain the dependence of the electron density on film thickness. However, Piper *et al* [35] and Cimalla *et al* [36] suggested that if dislocations at the interface act as a source of donors, as for InAs/GaP [67] and InAs/GaAs [68], this would give an effective mechanism with which to explain the thickness dependence of the single-field Hall effect results. The resulting model for electron density in InN films is shown schematically in figure 3(a), and is characterized by three contributions—I: the background 'bulk' density resulting from defects or impurities uniformly distributed throughout the film; II: surface electron accumulation; and III: donors due to dislocations, whose density falls off exponentially away from the interface.
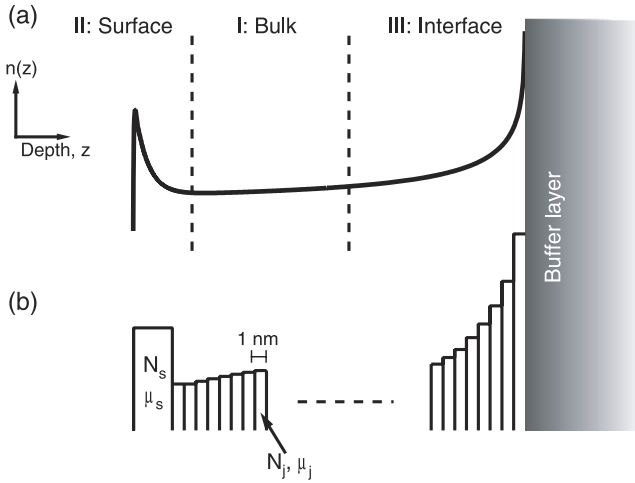
Figure 3. (a) Schematic representation of the 'three-region' model for conductivity in InN, indicating the I: bulk, II: surface, and III: interface contributions to the total electron concentration, n, as a function of depth. (b) Representation of the quantized layer model used for the full parallel conduction analysis described in the text.

Modelling of these three contributions was able to reproduce the film-thickness dependence of the carrier concentration determined from single-field Hall effect results for InN films grown on both GaN [35] and AlN [36, 69] buffer layers, but the analysis was performed assuming the same mobility for carriers in each region. To confirm this model, it is necessary to reanalyse the data incorporating varying mobilities of the different contributions, within a full parallel conduction treatment, as presented here. In this model, the sample is divided up into slabs of 1 nm thickness, shown schematically in figure 3(b). The volume density in the jth slab

$$n_j = n_b + D_j/C \tag{3}$$

where n_b is the background 'bulk' concentration considered previously, D_j is the areal density of dislocations in the slab, assumed to follow the relation $D(x) = A(10^{-\log_{10} x})$ with distance x from the interface [70], and C is the separation of charged centres along a dislocation. The constant A is treated as a fit parameter to reproduce the experimentally measured dislocation densities of 5.0×10^{10} cm^{-2} [62] and 2.2×10^{10} cm^{-2} [63] at 450 nm and 760 nm away from the InN/GaN interface, respectively. The mobility in the jth slab is given by

$$\mu_j^{-1} = \mu_{\mathrm{dis}_j}^{-1} + \mu_{\mathrm{ion}_j}^{-1} \tag{4}$$

from Matthiessen's rule, where the ionized impurity scattering is calculated as described above, and scattering from dislocations is included via the formalism of Look *et al* [62]

$$\mu_{\mathrm{dis}_j} = \frac{4(3^{2/3})eC^2 n_j^{2/3}}{\pi^{8/3}\hbar D_j} \left[1 + y(n_j)\right]^{3/2}, \tag{5}$$

where

$$y(n_j) = \frac{2(3^{1/3})\pi^{8/3}\hbar^2 \varepsilon n_j^{1/3}}{e^2 m^*}, \tag{6}$$

where $\varepsilon = 9.7$ is the static dielectric constant and m^* the effective mass. Although these relations assume parabolic band dispersion, conduction band non-parabolicity, important in InN, is approximately included by replacing the effective mass in these relations by the effective mass calculated at the Fermi level in each slab using Kane [71] non-parabolic relations and assuming a conduction band edge mass $m_0^* = 0.048m_0$ [72, 73]. The parallel conduction model introduced in equations (1) and (2) is extended to incorporate the surface, bulk and interface effects:

$$N_H \mu_H = N_s \mu_s + \sum_j (n_j \ell) \mu_j \tag{7}$$

$$N_H \mu_H^2 = N_s \mu_s^2 + \sum_j (n_j \ell) \mu_j^2 \tag{8}$$

where $\ell = 1$ nm is the thickness of each slab.

The calculated volume electron concentration and mobility, assuming singly charged scattering centres, a compensation ratio of 0.5, an impurity centre every three unit cells along a dislocation, and surface and bulk carrier parameters used above, are shown in figure 1 (solid lines). The thickness dependence of the volume electron density is well reproduced using this parallel conduction treatment, validating the results of previous studies [35, 36] where variations in mobility were not considered. Further, it allows a calculation of the Hall mobility, which, as shown in figure 1(b), exhibits good agreement with the measured values at sample thicknesses below ~1 μm. Above this, however, the experimental mobility is somewhat below that of the calculated values. Hsu *et al* [74] have shown that, while at high carrier concentrations, the mobility is limited virtually solely by coulomb scattering, at lower electron densities, other mechanisms such as polar optical and acoustic phonon scattering become important, reducing the mobility below that of the coulomb scattering limited value. For films thicker than ~1 μm, the electron density is relatively low, below 10^{18} cm^{-3}, and so it is likely that, in addition to coulomb and dislocation scattering, phonon scattering also becomes important, which would reduce the mobility below the calculated value, explaining the discrepancy between the calculated and measured values for thick films. Notwithstanding these slight discrepancies, the good general agreement between the calculated and measured electron concentrations and mobilities supports the three-region model for conductivity in InN, with the bulk, surface and particularly interface-related carriers all being important.

The highly n-type nature of an interface-related contribution is also supported by the infrared reflectivity measurements of Ishitani *et al* [75], who estimated a sheet density of ~10^{13} cm^{-2} electrons at the interface. Further, combined structural and electrical studies show a correlation between the TD density and the average (Hall) electron concentration in samples grown by both MBE [76] and MOVPE [77]. Variations in the interface-related electron density with buffer layers, growth polarity and growth conditions are also important. The 'excess' sheet density for zero thickness samples determined from single-field Hall effect results has

4

been shown to be slightly larger when using AlN rather than GaN buffer layers [37, 38], and for In-rather than N-polar InN samples, whilst the density of low-mobility electrons, not associated with the background 'bulk' carriers, in multiple-field Hall effect measurements has been shown to increase with decreasing In-flux during growth [78]. Any change in the sheet density of the surface electron accumulation with buffer layer, polarity, or growth conditions has been ruled out [29, 44, 79, 80], leaving the interface contribution as the only remaining plausible cause of these changes. Each increase in interface-related electron density can be correlated with an increase in the expected density of TDs, due to the larger lattice mismatch of InN with AlN than with GaN, or with differing polarity and growth conditions as previously inferred from x-ray diffraction studies [31].

4. Microscopic origins of the n-type conductivity

The above discussions have revealed the importance of the n-type conduction of InN originating from background donors, the surface and interface-related electrons. However, it must still be considered why each region exhibits such a tendency towards n-type conductivity, which is discussed in this section.

The background 'bulk' carriers must come from a uniform distribution of donor defects and/or impurities. Formation energies for the most important native defects and impurities are shown in figure 4, reproduced from the theoretical calculations of Stampfl *et al* [81] and Janotti and Van de Walle [82]. Typical Fermi level positions in InN, and the pinning position of the Fermi level at a clean InN surface are also shown. Note, for the Fermi level within the band gap, and indeed for all typical Fermi level positions in InN, donor native defects and impurities have the favourable charge state, indicated by the positive gradient of the formation energy. This is supported by experiment: native defects intentionally introduced into nominally undoped InN samples are donors [46]; Si and O act as effective n-type dopants in InN [49, 83, 84]; and hydrogen diffused into InN samples increases the conductivity [85, 86]. From the same considerations, native defects decorating, or impurities localized at, dislocations will also be donor-like, explaining the donor nature of the interface-related electron concentration in InN, in contrast to, for example, GaN [66].

Discriminating between which of these native defects is responsible for the unintentional n-type conductivity in InN has proved controversial. Due to the lower formation energies of impurities, such as oxygen and hydrogen, compared to native defects, these have been suggested as the dominant donors [30, 82]. However, in some cases, these do not appear to be present in sufficient quantities to account for the total conductivity [87], and native defects and dislocations were suggested as important sources of electrons. Hydrogen, being present in most growth environments, is certainly a promising candidate, at least for the background 'bulk' concentration of electrons. However, it should also be noted that interstitial hydrogen, with the lower formation energy of the hydrogen impurities, may not be stable at growth temperatures [82]. Additionally, an extrapolation of the
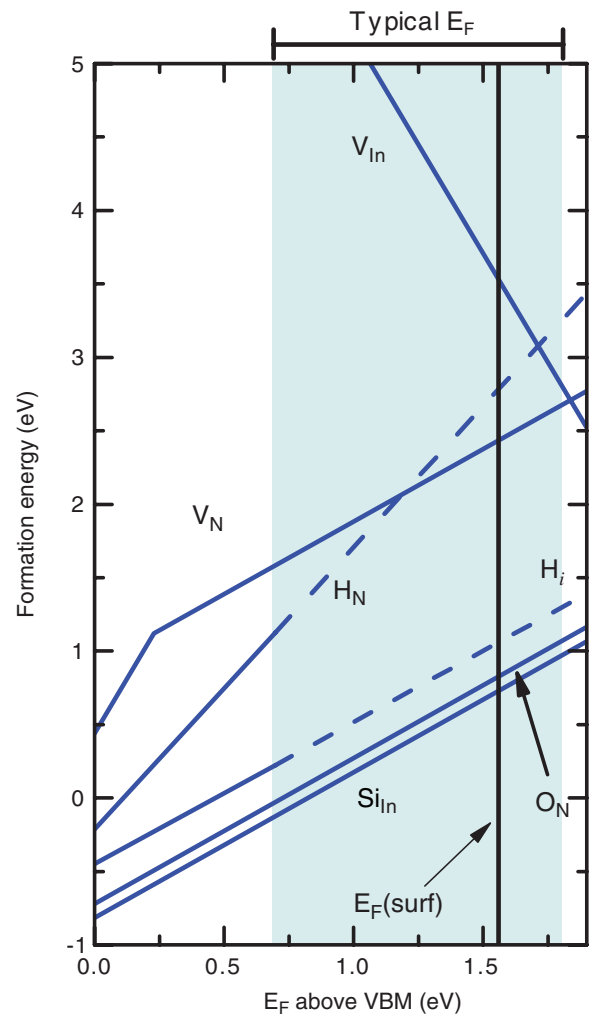

Figure 4. Formation energy as a function of Fermi level above the VBM for the most important native defects and impurities in InN, from the calculations of Stampfl *et al* [81] and Janotti and Van de Walle [82]. The dashed lines indicate an extrapolation of the calculated values of Janotti and Van de Walle [82] to higher Fermi levels (above the CBM). Typical Fermi level positions in InN are represented by shading, and the pinning position of the surface Fermi level [44] is also shown (vertical line).

(This figure is in colour only in the electronic version)

formation energy calculations of Janotti and Van de Walle [82] to Fermi levels above the CBM reveals that the formation energy for substitutional hydrogen and nitrogen vacancies may be expected to cross if H_N^{2+} remains the favourable charge state for substitutional hydrogen for Fermi levels well into the conduction band. At Fermi levels typical for InN samples, in particular at the surface where impurities are incorporated during growth, hydrogen impurities and native defects could both, therefore, be important.

Microscopic origins of the surface electron accumulation have also been investigated. Theoretical calculations predict that In-rich surface reconstructions involving In-adlayers are energetically favourable for all In chemical potential values [88], which have been experimentally confirmed under In-rich conditions from core-level photoemission [89] and ion scattering [90] measurements, and additionally from reflection

high energy electron diffraction intensity oscillations [33, 34]. In–In bonds in such an In-adlayer reconstruction have been predicted as a microscopic origin of the surface states giving rise to the electron accumulation in InN [91]. Native defects [46] and impurities [47] have also been suggested as possible mechanisms providing the donor surface charge in oxidized samples.

For the bulk, surface and interface-related carriers, an overriding bulk band structure explanation can also be employed to describe their tendency towards donor character. In InN, the CBM at the Γ-point lies particularly low compared to the average conduction band edge across the rest of the Brillouin zone [49, 92]. This causes the CBM to lie well below the so-called charge neutrality level (CNL), or branch-point energy [49]. Consequently, for Fermi levels up to around 1 eV above the CBM, native defects [46] and impurities such as hydrogen [93] preferentially have donor character. Additionally, the Fermi level generally pins close to, and in this case it must be slightly below, the CNL at the surface, leading to a number of unoccupied donor surface states, a positive surface charge, and consequently a downward band bending and accumulation of electrons in order to maintain charge neutrality [49, 94]. The position of the CBM relative to the CNL has been explained within the chemical trends of common-cation and common-anion semiconductors [49], and so, while the unintentional n-type conductivity in InN is certainly rather extreme, it cannot be considered anomalous.

5. Conclusions

The high unintentional n-type conductivity in InN has been considered. A 'three-region' model was discussed, including contributions from background donors, interface-related electrons and a surface electron accumulation layer. A parallel conduction analysis of this model was performed, incorporating both ionized impurity scattering and charged dislocation scattering, reproducing the thickness dependence of carrier concentration and mobility determined from single-field Hall effect measurements of a large number of samples. A number of microscopic candidates for the high donor concentrations in each region was introduced, although the overriding mechanism driving the high n-type conductivity can be understood as the charge neutrality level lying above the conduction band minimum in InN.

Acknowledgments

References

[1] Polyakov V M and Schwierz F 2006 *Appl. Phys. Lett.* **88** 032101
[2] Polyakov V M and Schwierz F 2006 *J. Appl. Phys.* **99** 113705
[3] Polyakov V M and Schwierz F 2006 *Semicond. Sci. Technol.* **21** 1651–5
[4] Bhuiyan A G, Hashimoto A and Yamamoto A 2003 *J. Appl. Phys.* **94** 2779–808
[5] Moss T S 1954 *Proc. Phys. Soc.* B **67** 775
[6] Burstein E 1954 *Phys. Rev.* **93** 632–3
[7] Tansley T L and Foley C P 1986 *J. Appl. Phys.* **59** 3241
[8] Lu H, Schaff W J, Hwang J, Wu H, Yeo W, Pharkya A and Eastman L F 2000 *Appl. Phys. Lett.* **77** 2548–50
[9] Davydov V Y *et al* 2002 *Phys. Status Solidi* b **229** R1–3
[10] Yamamoto A, Tanaka T, Koide K and Hashimoto A 2002 *Phys. Status Solidi* a **194** 510–4
[11] Wu J, Walukiewicz W, Yu K M, Ager J W III, Haller E E, Lu H, Schaff W J, Saito Y and Nanishi Y 2002 *Appl. Phys. Lett.* **80** 3967–9
[12] Davydov V *et al* 2002 *Phys. Status Solidi* b **230** R4–6
[13] Davydov V *et al* 2002 *Phys. Status Solidi* b **234** 787–95
[14] Wu J, Walukiewicz W, Shan W, Yu K M, Ager J W III, Li S X, Haller E E, Lu H and Schaff W J 2003 *J. Appl. Phys.* **94** 4457–60
[15] Wu J, Walukiewicz W, Yu K M, Shan W, Ager J W III, Haller E E, Lu H, Schaff W J, Metzger W K and Kurtz S 2003 *J. Appl. Phys.* **94** 6477–82
[16] Nakamura S 1998 *Science* **281** 956–61
[17] Ponce F A and Bour D P 1997 *Nature* **386** 351–9
[18] Chichibu S F *et al* 2006 *Nat. Mater.* **5** 810
[19] Schubert E F and Kim J K 2005 *Science* **308** 1274–8
[20] Ascázubi R, Wilke I, Denniston K, Lu H and Schaff W J 2004 *Appl. Phys. Lett.* **84** 4810–2
[21] Cimalla V, Pradarutti B, Matthus G, Brckner C, Riehemann S, Notni G, Nolte S, Tnnermann A, Lebedev V and Ambacher O 2007 *Phys. Status Solidi* b **244** 1829–33
[22] Ahn H, Ku Y P, Chuang C H, Pan C L, Lin H W, Hong Y L and Gwo S 2008 *Appl. Phys. Lett.* **92** 102103
[23] Ahn H, Ku Y P, Wang Y C, Chuang C H, Gwo S and Pan C L 2007 *Appl. Phys. Lett.* **91** 132108
[24] Lu H, Schaff W J and Eastman L F 2004 *J. Appl. Phys.* **96** 3577–9
[25] Chen C F, Wu C L and Gwo S 2006 *Appl. Phys. Lett.* **89** 252109
[26] Lu Y S, Huang C C, Yeh J A, Chen C F and Gwo S 2007 *Appl. Phys. Lett.* **91** 202109
[27] Lu Y S, Ho C L, Yeh J A, Lin H W and Gwo S 2008 *Appl. Phys. Lett.* **92** 212102
[28] Lu H, Schaff W J, Eastman L F, Wu J, Walukiewicz W, Look D C and Molnar R J 2003 *Mater. Res. Soc. Symp. Proc.* **743** L4.10.1–6
[29] Schaff W J, Lu H, Eastman L F, Walukiewicz W, Yu K M, Keller S, Kurtz S, Keyes B and Gevilas L 2004 *State-of-the-Art Program on Compound Semiconductors XLI and Nitride and Wide Bandgap Semiconductors for Sensors, Photonics, and Electronics V* (*The Electrochemical Society Proceedings Series* vol 2004–06) ed H M Ng and A G Baca (Pennington, NJ: Electrochemical Society) pp 358–71 Honolulu, Hawaii, October 2004
[30] Gallinat C S, Koblmüller G, Brown J S, Bernardis S, Speck J S, Chern G D, Readinger E D, Shen H and Wraback M 2006 *Appl. Phys. Lett.* **89** 032109
[31] Koblmüller G, Gallinat C S, Bernardis S, Speck J S, Chern G D, Readinger E D, Shen H and Wraback M 2006 *Appl. Phys. Lett.* **89** 071902
[32] Wang X, Che S B, Ishitani Y and Yoshikawa A 2006 *Japan. J. Appl. Phys.* **45** L730–3
[33] Gallinat C S, Koblmüller G, Brown J S and Speck J S 2007 *J. Appl. Phys.* **102** 064907
[34] Koblmüller G, Gallinat C S and Speck J S 2007 *J. Appl. Phys.* **101** 083516
[35] Piper L F J, Veal T D, McConville C F, Lu H and Schaff W J 2006 *Appl. Phys. Lett.* **88** 252109

[36] Cimalla V, Lebedev V, Morales F M, Goldhahn R and Ambacher O 2006 *Appl. Phys. Lett.* **89** 172109
[37] Lu H, Schaff W J, Eastman L F and Wood C 2002 *Mater. Res. Soc. Symp. Proc.* **693** I1.5
[38] Lu H, Schaff W J, Eastman L F and Stutz C E 2003 *Appl. Phys. Lett.* **82** 1736–8
[39] Swartz C, Tompkins R, Giles N, Myers T, Lu H, Schaff W and Eastman L 2004 *J. Cryst. Growth* **269** 29–34
[40] Swartz C H, Tomkins R P, Myers T H, Lu H and Schaff W J 2005 *Phys. Status Solidi* c **2** 2250–3
[41] Fehlberg T B, Umana-Membreno G A, Nener B D, Parish G, Gallinat C S, Koblmüller G, Rajan S, Bernardis S and Speck J S 2006 *Japan. J. Appl. Phys.* **41** L1090–2
[42] Noguchi M, Hirakawa K and Ikoma T 1991 *Phys. Rev. Lett.* **66** 2243–6
[43] Mahboob I, Veal T D, McConville C F, Lu H and Schaff W J 2004 *Phys. Rev. Lett.* **92** 036804
[44] King P D C *et al* 2007 *Appl. Phys. Lett.* **91** 092101
[45] Piper L F J, Veal T D, Mahboob I, McConville C F, Lu H and Schaff W J 2004 *Phys. Rev.* B **70** 115333
[46] Li S X, Yu K M, Wu J, Jones R E, Walukiewicz W, Ager J W III, Shan W, Haller E E, Lu H and Schaff W J 2005 *Phys. Rev.* B **71** 161201
[47] Cimalla V, Ecke G, Niebelschtz M, Ambacher O, Goldhahn R, Lu H and Schaff W J 2005 *Phys. Status Solidi* c **2** 2254–7
[48] Veal T D, Jefferson P H, Piper L F J, McConville C F, Joyce T B, Chalker P R, Considine L, Lu H and Schaff W J 2006 *Appl. Phys. Lett.* **89** 202110
[49] King P D C *et al* 2008 *Phys. Rev.* B **77** 045316
[50] Calleja E, Grandal J, Sánchez-Garcia M A, Niebelschütz M, Cimalla V and Ambacher O 2007 *Appl. Phys. Lett.* **90** 262110
[51] Lazić S, Gallardo E, Calleja J M, Agulló-Rueda F, Grandal J, Sánchez-Garcia M A, Calleja E, Luna E and Trampert A 2007 *Phys. Rev.* B **76** 205319
[52] Wu C L, Lee H M, Kuo C T, Chen C H and Gwo S 2008 *Phys. Rev. Lett.* **101** 106803
[53] Huijser A and Van Laar J 1975 *Surf. Sci.* **52** 202–10
[54] Spicer W E, Lindau I, Gregory P E, Garner C M, Pianetta P and Chye P W 1976 *J. Vac. Sci. Technol.* **13** 780–5
[55] Rangel-Kuoppa V T, Suihkonen S, Sopanen M and Lipsanen H 2006 *Japan. J. Appl. Phys.* **45** 36–9
[56] Petritz R L 1958 *Phys. Rev.* **110** 1254–62
[57] Jones R E, Yu K M, Li S X, Walukiewicz W, Ager J W III, Haller E E, Lu H and Schaff W J 2006 *Phys. Rev. Lett.* **96** 125505
[58] Zawadzki W 1974 *Adv. Phys.* **23** 435–522
[59] Jones R E, Li S X, Hsu L, Yu K M, Walukiewicz W, Lillental-Weber Z, Ager J W III, Haller E E, Lu H and Schaff W J 2006 *Physica* B **376** 436–9
[60] Anderson P A, Swartz C H, Carder D, Reeves R J, Durbin S M, Chandril S and Myers T H 2006 *Appl. Phys. Lett.* **89** 184104
[61] Veal T D, Piper L F J, Schaff W J and McConville C F 2006 *J. Cryst. Growth* **288** 268–72
[62] Look D C, Lu H, Schaff W J, Jasinski J and Liliental-Weber Z 2002 *Appl. Phys. Lett.* **80** 258–60
[63] Lu C J, Bendersky L A, Lu H and Schaff W J 2003 *Appl. Phys. Lett.* **83** 2817–9

[64] Lebedev V, Cimalla V, Pezoldt J, Himmerlich M, Krischok S, Schaefer J A, Ambacher O, Morales F M, Lozano J G and González D 2006 *J. Appl. Phys.* **100** 094902
[65] Liu Y, Cai Y, Zhang L, Xie M H, Wang N, Zhang S B and Wu H S 2008 *Appl. Phys. Lett.* **92** 231907
[66] Look D C and Sizelove J R 1999 *Phys. Rev. Lett.* **82** 1237–40
[67] Gopal V, Kvam E P, Chin T P and Woodall J M 1998 *Appl. Phys. Lett.* **72** 2319–21
[68] Yamaguchi H, Sudijono J L, Joyce B A, Jones T S, Gatzke C and Stradling R A 1998 *Phys. Rev.* B **58** R4219–22
[69] Lebedev V, Cimalla V, Baumann T, Ambacher O, Morales F M, Lozano J G and González D 2006 *J. Appl. Phys.* **100** 094903
[70] Jasinski J and Liliental-Weber Z 2002 *J. Electron. Mater.* **31** 429
[71] Kane E O 1957 *J. Phys. Chem. Solids* **1** 249
[72] Hofmann T, Chavdarov T, Darakchieva V, Lu H, Schaff W J and Schubert M 2006 *Phys. Status Solidi* c **3** 1854–7
[73] Nag B R 2003 *Phys. Status Solidi* b **237** R1–2
[74] Hsu L, Jones R E, Li S X, Yu K M and Walukiewicz W 2007 *J. Appl. Phys.* **102** 073705
[75] Ishitani Y, Fujiwara M, Wang X, Che S B and Yoshikawa A 2008 *Appl. Phys. Lett.* **92** 251901
[76] Wang X, Che S B, Ishitani Y and Yoshikawa A 2007 *Appl. Phys. Lett.* **90** 151901
[77] Wang H *et al* 2008 *J. Phys. D: Appl. Phys.* **41** 135403
[78] Fehlberg T B, Gallinat C S, Umana-Membreno G A, Koblmüller G, Nener B D, Speck J S and Parish G 2008 *J. Electron. Mater.* **37** 593–6
[79] Veal T D, Piper L F J, Mahboob I, Lu H, Schaff W J and McConville C F 2005 *Phys. Status Solidi* c **2** 2246–9
[80] King P D C, Veal T D, Gallinat C S, Koblmüller G, Bailey L R, Speck J S and McConville C F 2008 *J. Appl. Phys.* **104** 103703
[81] Stampfl C, Van de Walle C G, Vogel D, Krüger P and Pollmann J 2000 *Phys. Rev.* B **61** R7846–9
[82] Janotti A and Van de Walle C G 2008 *Appl. Phys. Lett.* **92** 032104
[83] Higashiwaki M, Inushima T and Matsui T 2003 *Phys. Status Solidi* b **240** 417–20
[84] Kim J, Ikenaga E, Kobata M, Takeuchi A, Awaji M, Makino H, Chen P, Yamamoto A, Matsuoka T and Miwa D 2006 *Appl. Surf. Sci.* **252** 5602–6
[85] Losurdo M, Giangregorio M M, Bruno G, Kim T H, Choi S, Brown A S, Pettinari G, Capizzi M and Polimeni A 2007 *Appl. Phys. Lett.* **91** 081917
[86] Pettinari G *et al* 2008 *Phys. Rev.* B **77** 125207
[87] Wu J *et al* 2004 *Appl. Phys. Lett.* **84** 2805–7
[88] Segev D and Van de Walle C G 2007 *Surf. Sci.* **601** L15–8
[89] Veal T D *et al* 2007 *Phys. Rev.* B **76** 075313
[90] Veal T D, King P D C, Walker M, McConville C F, Lu H and Schaff W J 2007 *Physica* B **401/402** 351–4
[91] Segev D and Van de Walle C G 2006 *Europhys. Lett.* **76** 305–11
[92] Furthmüller J, Hahn P H, Fuchs F and Bechstedt F 2005 *Phys. Rev.* B **72** 205106
[93] Van de Walle C G and Neugebauer J 2003 *Nature* **423** 626–8
[94] Mahboob I, Veal T D, Piper L F J, McConville C F, Lu H, Schaff W J, Furthmüller J and Bechstedt F 2004 *Phys. Rev.* B **69** 201307(R)